INFECTION AND IMMUNITY, July 2007, p. 3434–3444 Vol. 75, No. 7
0019-9567/07/$08.00+0 doi:10.1128/IAI.01345-06

Transcriptional Profiling of *Bacillus anthracis* during Infection of Host Macrophages[▽]†

Nicholas H. Bergman,[1,2]* Erica C. Anderson,[1] Ellen E. Swenson,[1] Brian K. Janes,[1] Nathan Fisher,[1] Matthew M. Niemeyer,[1] Amy D. Miyoshi,[1] and Philip C. Hanna[1]

Department of Microbiology & Immunology[1] and Bioinformatics Program,[2] University of Michigan Medical School, Ann Arbor, Michigan 48109

Received 22 August 2006/Returned for modification 3 October 2006/Accepted 18 April 2007

The interaction between *Bacillus anthracis* and the mammalian phagocyte is one of the central stages in the progression of inhalational anthrax, and it is commonly believed that the host cell plays a key role in facilitating germination and dissemination of inhaled *B. anthracis* spores. Given this, a detailed definition of the survival strategies used by *B. anthracis* within the phagocyte is critical for our understanding of anthrax. In this study, we report the first genome-wide analysis of *B. anthracis* gene expression during infection of host phagocytes. We developed a technique for specific isolation of bacterial RNA from within infected murine macrophages, and we used custom *B. anthracis* microarrays to characterize the expression patterns occurring within intracellular bacteria throughout infection of the host phagocyte. We found that *B. anthracis* adapts very quickly to the intracellular environment, and our analyses identified metabolic pathways that appear to be important to the bacterium during intracellular growth, as well as individual genes that show significant induction in vivo. We used quantitative reverse transcription-PCR to verify that the expression trends that we observed by microarray analysis were valid, and we chose one gene (GBAA1941, encoding a putative transcriptional regulator) for further characterization. A deletion strain missing this gene showed no phenotype in vitro but was significantly attenuated in a mouse model of inhalational anthrax, suggesting that the microarray data described here provide not only the first comprehensive view of how *B. anthracis* survives within the host cell but also a number of promising leads for further research in anthrax.

Bacillus anthracis, the causative agent of anthrax, has come under increased scrutiny in recent years because of its potential role as a bioweapon (35). In the environment, *B. anthracis* exists primarily as a metabolically dormant endospore, and in this morphology the bacterium is both highly infectious and resistant to a wide range of harsh conditions (42). When the spores are inhaled, they reach the alveolar spaces of the lung, where they are efficiently taken up by resident phagocytes (5, 9, 48). It is commonly believed that the host cells then migrate across the alveolocapillary barrier, transporting the intracellular bacteria into the lymphatic system (26, 40). During this time, the bacteria germinate, transforming from spores into vegetative bacilli, which begin to replicate within the phagocytes (15, 50). Eventually, the bacteria kill the phagocytes and escape into the extracellular environment, and the resulting sepsis ultimately leads to death of the host (23, 24, 43, 52, 57).

Since the progression of anthrax is typically quite rapid once the systemic phase of the infection begins (16, 24), successful intervention depends on early diagnosis and treatment. Given this fact, it is particularly important from a therapeutic standpoint that the early events in anthrax are well understood. Most of these events occur within the context of the host phagocyte, and in recent years a number of studies have focused on the interaction between *B. anthracis* and the host cell (9, 13, 40, 45, 46, 53). Although considerable progress has been made in understanding the host side of this interaction, relatively little is known about how *B. anthracis* survives within the phagocyte and establishes a productive infection.

In this study, we sought to approach these problems in a global way and establish a knowledge base that would allow us to begin to understand the pathogenic strategies employed by *B. anthracis* within the host. With these goals in mind, we used DNA microarrays to perform whole-genome transcriptional profiling of bacteria isolated from within murine macrophages at various time points during infection. We characterized the gene expression patterns occurring within *B. anthracis* throughout its entire interaction with the host cell, from uptake and germination through the death of the macrophage and escape of the bacteria. Our analyses identified several pathways and functions that appear to be important for bacterial survival within the host cell and thus may be useful targets in future drug development efforts. We also identified a large number of *B. anthracis* genes (both well studied and previously uncharacterized) that are highly induced during growth within the host cell and appear to be possibly virulence related. One uncharacterized gene, a putative transcriptional regulator belonging the MarR family, was chosen for further study, and we found that although a deletion strain missing this locus had no discernible phenotype in vitro, it was significantly attenuated in terms of its ability to cause disease in a mouse model of inhalational anthrax. Overall, our data provide global insights into how *B. anthracis* adapts to the environment within the

* Corresponding author. Mailing address: Bioinformatics Program and Department of Microbiology & Immunology, University of Michigan Medical School, 6706 Medical Sciences Bldg. II, 1150 W. Medical Center Dr., Ann Arbor, MI 48109-0620. Phone: (734) 615-2154. Fax: (734) 764-3562. E-mail: niber@umich.edu.

† Supplemental material for this article may be found at http://iai.asm.org/.

▽ Published ahead of print on 30 April 2007.

macrophage, as well as a variety of promising new leads for further research in anthrax.

MATERIALS AND METHODS

Bacterial and murine cell cultures. All work described in this report was done using the Sterne $34F_2$ strain ($pXO1^+$ $pXO2^-$) of *B. anthracis*. This strain was chosen because the *B. anthracis* poly-D-glutamic acid capsule, produced by enzymes encoded in the pXO2 plasmid, is not known to play a major role in virulence until the later stages of anthrax (when it becomes a major factor in facilitating systemic spread of the bacilli) (17). The capsule's role during the early stages of infection, including the initial interaction with the host macrophage, remains uncertain (20), and thus the Sterne strain is commonly used to study these early interactions because unlike $pXO1^+$ $pXO2^+$ strains, it does not require a BSL3 environment. Initial spore stocks were prepared as follows. A single *B. anthracis* culture was grown overnight at 37°C, and then 1 ml was used to inoculate 500 ml of modified G medium [0.2% yeast extract with a final amino acid concentration of roughly 14 mM, 0.17 mM $CaCl_2$, 2.87 mM K_2HPO_4, 0.81 mM $MgSO_4$, 0.24 mM $MnSO_4$, 17 μM $ZnCl_2$, 20 μM $CuSO_4$, 1.8 μM $FeCl_3$, and 15.5 mM $(NH_4)_2SO_4$, adjusted to pH 7.2] as described previously (15, 29, 36). Bacterial growth was measured by spectrophotometry at 600 nm. Progress through sporulation was monitored microscopically by scoring for the presence of phase-bright spores and by measuring the percentage of cells in a culture that were capable of surviving an extended heat treatment (65°C for 30 min). Spores were purified as described previously (38). The resulting spore stock was >99% pure when it was assayed by heat sensitivity assays, and it contained no appreciable vegetative debris when it was examined microscopically. The murine macrophage-like RAW 264.7 cell line (ATCC TIB-71) was maintained in Dulbecco's modified Eagle's medium with 10% fetal bovine serum (Gibco-BRL) at 37°C with 5% CO_2 in a humidified incubator. In all experiments, RAW 264.7 cells were passaged fewer than 10 times prior to infection.

Infection conditions. Infections were done as described by Bergman et al. (7). Briefly, 24 h prior to infection, RAW 264.7 cells were counted and switched from Dulbecco's modified Eagle's medium–10% fetal bovine serum to minimal essential medium with 10% horse serum, as this combination has been shown to inhibit outgrowth of extracellular spores. Cells were seeded at a concentration of 3×10^7 cells per 30 ml of medium in 150-cm^2 cell culture flasks and cultured overnight at 37°C. Infections were begun by removing the medium and adding 15 ml (0.5 volume) of fresh minimal essential medium–10% horse serum containing *B. anthracis* Sterne $34F_2$ spores at a multiplicity of infection of 10:1. Infections were monitored microscopically and progressed as described previously (7).

RNA extraction. In the initial experiments, total RNA (including both eukaryotic and prokaryotic RNA species) was extracted from infected macrophages by scraping the cells, centrifuging the preparation for 3 min at $2,500 \times g$, and then proceeding as described previously (6). Briefly, the cell pellet (containing both macrophages and bacteria) was incubated in boiling lysis buffer (2% sodium dodecyl sulfate, 16 mM EDTA [pH 8.0], 20 mM NaCl) for 3 min. Following lysis, the mixture was extracted successively in phenol (65°C, twice), phenol (22°C), a 25:24:1 mixture of phenol, $CHCl_3$, and isoamyl alcohol, and finally $CHCl_3$-isoamyl alcohol (24:1). RNA was then precipitated by addition of 2.5 volumes of 100% ethanol and incubation at −20°C. Pellets were washed with 70% ethanol and resuspended in 200 μl H_2O. The resulting RNA was further purified using an RNeasy kit (QIAGEN), and concentrations were measured by UV spectrophotometry. RNA quality was assessed by measuring the ratio of absorbance at 260 nm to absorbance at 280 nm, as well as by visualization with an Agilent 2100 Bioanalyzer or in denaturing agarose gels. Gels were also used to monitor the levels of contaminating murine RNA.

In later experiments, the procedure described above was modified to include a differential lysis step so that the amount of contaminating eukaryotic RNA was minimized. In these cases, at the appropriate time point culture flasks containing infected macrophages were decanted, and the culture medium was replaced with a 4% solution of saponin (Sigma) in sterile phosphate-buffered saline. The cells were incubated with gentle rocking at room temperature for ~3 min, during which the cellular monolayer could easily be seen sloughing from the surface of the culture flask. Following this incubation, the solution was transferred to a centrifuge tube and spun at a very low speed ($100 \times g$) for 1 min to pellet the bacteria (these parameters were sufficient to yield a sizable pellet while keeping much of the eukaryotic cell debris in the supernatant). After this, RNA isolation proceeded as described above, beginning with the incubation in boiling lysis buffer. Finally, in all but the initial experiments, further enrichment of bacterial RNA in mixed samples was done using a MicrobEnrich kit (Ambion) according to the manufacturer's instructions.

Control experiments verified that incubation in 4% saponin for 3 to 5 min did not affect the viability of *B. anthracis* spores or vegetative cells (data not shown). In addition, when comparing the transcriptional profiles of RNA samples isolated before and after incubation in saponin, we found that these incubation conditions caused no appreciable change in bacterial gene expression (expression of ~0.1% of all genes changed by a statistically significant measure [data not shown]). This is consistent with studies of other bacterial pathogens, where saponin has also been used to specifically lyse host cells and has been shown to have no noticeable effect on bacterial gene expression (18).

Microarray design. The *B. anthracis* microarray used in this study was developed based on the Affymetrix GeneChip platform. The arrays contained 25-mer probes corresponding to each of the 5,815 open reading frames in the *B. anthracis* Ames Ancestor sequence (GB accession numbers NC_007530, NC_007322, and NC_007322, corresponding to the chromosome, pXO1, and pXO2, respectively) at a density of 18 probes per gene. Further details, as well as probe sequences, are available upon request. The arrays were described recently in a comprehensive study of the complete *B. anthracis* life cycle in vitro (6), and during the course of that study data obtained from these arrays were validated by comparison to quantitative reverse transcription (RT)-PCR data, as well as to microarray data generated using other array systems. In all cases the data resulting from the GeneChips described here were consistent with data generated using other methods.

Microarray sample processing and data collection. RNA samples were reverse transcribed, and the corresponding cDNA samples were purified, fragmented, and labeled according to Affymetrix-recommended protocols (available at http://www.affymetrix.com/support/downloads/manuals/expression_s3_manual.pdf) at the UM Comprehensive Cancer Center Microarray Core Facility. Hybridization to the *B. anthracis* GeneChips and scanning of the arrays were also done according to standard Affymetrix protocols. At this point, several quality control steps were performed in order to ensure that the raw data were of sufficient quality to proceed. First, the distributions of perfect match probe intensities for each chip were compared, since the robust multichip average procedure used for normalization and background correction over multiple chips is based on the assumption that these distributions are very similar. Once this assumption was verified, a plot of average probe intensity versus position within a gene was generated for each sample. This plot shows whether there is a systematic skew within a given data set toward probes that lie near the end of each gene, which would indicate a high level of RNA degradation or a problem with the RT step. Once we verified that all the samples showed similar 5′-3′ profiles, we used the robust multichip average method to subtract the background, normalize the data, and compute a single probe set summary for each gene (8, 32, 33). Principal-component analysis verified that biological replicates were very similar to each other and formed relatively tight clusters (data not shown).

Data analysis. Statistical analysis of microarray data, including sample distance calculations, matrix construction, and significance analysis of microarrays (SAM), was done using the TM4 suite of programs (http://www.tm4.org/ [51]), the Analyze-It statistical software package (Analyze-It Software, Ltd., Leeds, United Kingdom) for Microsoft Excel (Microsoft, Redmond, WA), and the Prism 4 statistical software package (GraphPad Software, San Diego, CA). Note that in all cases, SAM was done with the following criteria for differentially expressed genes: a false discovery rate (FDR) of <0.001 and >2.00-fold expression change (with the aim of combining a relatively permissive fold change cutoff with a reasonably strict FDR in attempting to minimize both false positives and false negatives). Pathway analysis of array data was done using the EASE algorithm (30) as implemented within the TM4-MeV program, as well as a set of GO and TIGRFAM tables compiled from the TIGR Comprehensive Microbial Resource (http://www.tigr.org/CMR/). The significance of overrepresentations was assessed using the Fisher exact text.

Quantitative RT-PCR. Quantitative RT-PCR was performed as described previously (44). Briefly, "in vitro" RNA was collected as described previously (6) from a log-phase culture at an optical density at 600 nm of ~0.3 growing with rapid shaking in modified G medium, and "in vivo" RNA was collected using essentially the same procedure from infected macrophages 4 h postinfection (without the differential lysis or MicrobEnrich steps described above). cDNA was prepared from each RNA sample using random primers and Invitrogen SuperScript II reverse transcriptase. RT-PCRs were performed in duplicate in a 384-well plate at the University of Michigan Comprehensive Cancer Center cDNA Core Facility using an ABI Prism 7900 HT SDS with the SDS Software version 2.0 sequence detection system, an annealing temperature of 56.4°C, and extension at 72°C for 1 min for 35 cycles. Primer sequences are available upon request and were designed to amplify a 160- to 180-bp product in each case. The amplification efficiencies were roughly equivalent across all primer sets. Control reactions were performed to verify that there was no genomic DNA contamination (that is, the threshold cycle [C_T] for detection in the control without RT was

at least four cycles above the C_T in the test reaction). Normalization of C_T values was done relative to the signal obtained from reactions amplifying a portion of the GBAA2365 transcript; the expression level of this gene has been shown previously to vary less than twofold across the entire *B. anthracis* life cycle (6), and the microarray experiments described in this study suggested that its expression levels are very similar (within 10%) during growth in vitro and in vivo. After normalization, the fold change between "in vivo" and "in vitro" was calculated as follows: $2^{(\bar{X}_{C_T[\text{in vivo}]} - \bar{X}_{C_T[\text{in vitro}]})}$. Statistical analyses, including Deming linear regression, were done using the Prism 4 statistical software package (GraphPad).

Construction of a *B. anthracis* ΔGBAA1941 deletion strain. The ΔGBAA1941 mutant used in this work has a markerless, in-frame deletion in which 384 of 444 bp (86.5%) of the gene has been deleted. The mutant allele contains the predicted initial 10 codons of the gene (including the initiation codon), a short insert sequence containing three stop codons, and the recognition sequence for two restriction endonucleases, BamHI and SmaI (insert sequence, TAATAGTGAG GATCCCCCGGG), followed by the predicted terminal 10 codons (including the stop codon). Standard PCR methods (primer sequences available upon request) were used to generate a DNA fragment that contained this sequence flanked upstream and downstream by approximately 500 bp of sequence homologous to the region of the *B. anthracis* chromosome containing GBAA1941. This construct was cloned using a pCR8/GW/TOPO TA cloning kit (Invitrogen) according the manufacturer's instructions, and the DNA sequence was verified by sequencing at the University of Michigan Medical School DNA Sequencing Core Facility. The construct was then moved into the allelic exchange vector pBKJ258 (34, 37), and the integrated mutant allele was isolated on the chromosome using methods described previously (34). It should be noted that this mutant is otherwise isogenic to the starting wild-type strain. PCR (using primers that anneal outside the sequence used in construction of the mutant) was used to show that the region contained the predicted 363-bp deletion and that the pXO1 plasmid was intact in the isolated mutant.

Intratracheal inoculation of DBA/2 mice. Mouse infection was done essentially as described previously (21). Briefly, DBA/2 mice were anesthetized by intraperitoneal injection of ketamine (2.5 mg/mouse) and xylazine (0.1 mg/mouse), and a small incision was made through the skin over the trachea. A 30-gauge needle was inserted into the trachea, and a 30-μl inoculum containing 1.5×10^4 *B. anthracis* $34F_2$ or ΔGBAA1941 endospores suspended in deionized, distilled water was dispensed into the lungs. Following inoculation, the skin was closed with cyanoacrylate adhesive. Aliquots of the inoculum were plated before and after inoculation to monitor the number of CFU delivered. All mouse experiments were done using protocols approved by the University of Michigan Committee on the Use and Care of Animals. Postmortem necropsies were performed on representative mice in order to verify that *B. anthracis* was the only species detected in blood or lung samples, and PCR was used to verify that the pXO1 plasmid had not been lost during the course of passaging in the mouse. Survival curves were visualized using the Kaplan-Meier survival analysis method implemented within the Prism 4 software package (GraphPad), and curves were compared using the log rank test implemented within that program.

Data and reagent availability. All microarray data described in this study are freely available from the NIAID Administrative Resource for Biodefense Proteomics Research Programs (http://www.proteomicsresource.org) or from the ArrayExpress database (http://www.ebi.ac.uk/arrayexpress) (accession number E-MEXP-1036). The custom *B. anthracis* microarrays can be purchased (for research purposes) from Affymetrix with permission from the developers; further information can be obtained by contacting us.

RESULTS AND DISCUSSION

In order to better understand the ways in which *B. anthracis* interacts with the host phagocyte during infection, we used DNA microarrays to characterize *B. anthracis* gene expression on a global scale at various points throughout infection of phagocytes. To do this, we took advantage of a widely used model infection system in which the Sterne $34F_2$ strain of *B. anthracis* is used to infect the murine RAW 264.7 macrophage-like cell line. A recent study by our group defined the timing of infection for this system in some detail, and all infections in the current study were done as described by Bergman et al. (7). Briefly, when spores were added to the macrophage culture, they were efficiently phagocytosed, and germinating bacterial cells were visualized within macrophages roughly 1 h after inoculation. After 3 h bacterial replication could be observed, and after 6 h further growth had occurred and the majority of the macrophages were dead or dying. As we noted in our previous study, the medium used in these experiments (minimal essential medium plus 10% horse serum) did not support growth of *B. anthracis*, and extracellular vegetative cells were not observed until late in the experiment (between 5 and 6 h postinfection), when they could be seen in and around dying macrophages (7).

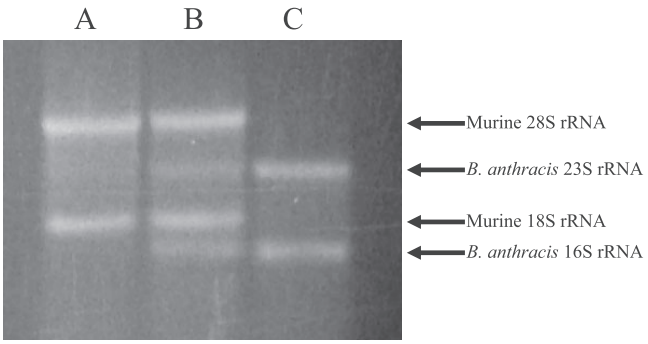

FIG. 1. Gel electrophoresis of RNA samples isolated from *B. anthracis*-infected RAW 264.7 cells. Lane A contained a typical sample of total RNA isolated from an infected culture using a simple extraction procedure, and only the eukaryotic 28S and 18S rRNA species are visible (arrows indicate eukaryotic [28S and 18S] and prokaryotic [23S and 16S] rRNA bands). Lane B contained a sample prepared using the differential lysis-based protocol described in the text, and both eukaryotic and prokaryotic rRNA bands are visible. Lane C contained RNA prepared like that in lane B and further purified using the MicrobEnrich kit (Ambien) to remove eukaryotic RNA. All lanes contained equivalent amounts of RNA (roughly 5 μg).

Purification of *B. anthracis* RNA from within infected macrophages. Although total RNA could be easily isolated from infected macrophages using a simple extraction procedure (essentially harvesting the macrophages by scraping and centrifuging and then proceeding as described previously [6]), we found that mixed samples prepared in this way generally contained overwhelming amounts of contaminating murine RNA (Fig. 1, lane A, where only the eukaryotic rRNA bands are visible). This level of contamination made microarray analysis of the bacterial component impossible due to the extremely high background (E. C. Anderson and N. H. Bergman, unpublished data), so we explored different ways of isolating RNA from infected cells such that the contaminating murine component would be minimized. Our main strategy in overcoming this obstacle exploited the observation that under most conditions, macrophages lyse much more readily than *B. anthracis* cells. In pilot experiments we found that a short (3-min) incubation in a solution of saponin (4% in sterile phosphate-buffered saline) efficiently lysed the macrophages and released the intracellular bacteria, and control experiments showed that these conditions did not affect bacterial viability or gene expression (see Materials and Methods). Based on these preliminary results, we added a differential lysis step to our standard RNA extraction protocol, such that infected macrophages were incubated in 4% saponin for 3 min, after which the entire mixture was centrifuged at low speed for 1 min to pellet the bacterial cells. RNA extraction of these pellets yielded samples

that were much less contaminated (Fig. 1, lane B, in which both bacterial and eukaryotic rRNA bands are visible). Although these samples still had a significant eukaryotic component, addition of a final purification step using the commercially available MicrobEnrich kit allowed us to specifically remove the majority of the remaining eukaryotic RNA and produce samples that were significantly enriched in bacterial RNA (Fig. 1, lane C). Note that in our final protocol, both the differential lysis step and the final purification with the MicrobEnrich kit were required; the former is limited in the overall purity obtained, while the latter is limited by the overall RNA capacity and thus requires some prior enrichment of the input RNA in order to attain acceptable yields. The apparent purity of the samples produced by our final protocol suggested that they would be amenable to microarray analysis, and this was verified in pilot experiments that showed that the average background levels, probe intensity distributions, and 3′/5′ ratios for these samples were all very similar to those of *B. anthracis* RNA samples collected from pure bacterial cultures (data not shown).

Using the RNA purification procedure outlined above, we isolated bacterial RNA from *B. anthracis*-infected macrophages at 1, 2, 3, 4, 5, and 6 h postinoculation. The progress of the infection was monitored via microscopy and was essentially identical to the general time frame reported previously (7). As noted above, we did not observe extracellular growth of *B. anthracis* until late in the infection (between 5 and 6 h postinfection), when the bacilli appeared to be escaping from dying macrophages. Each of the samples collected (at least three independent biological replicates at a given time point and a total of 23 samples) was subjected to microarray analysis using a custom Affymetrix *B. anthracis* GeneChip described and tested recently by Bergman et al. (6).

Changes in *B. anthracis* gene expression during macrophage infection. One of the larger questions that we hoped to address in this study was the issue of how much *B. anthracis* gene expression changes during infection of the host phagocyte. Our previous work investigating macrophage gene expression (using the same model infection system and time frame) had shown that host mRNA expression patterns change significantly several times during infection (7), and we anticipated that there might be analogous shifts in *B. anthracis* expression, perhaps as the bacterium makes metabolism- or virulence-associated adjustments to its transcription profile as it grows within the host cell. To test this possibility directly, we calculated the overall relatedness (expressed as a Pearson correlation) for each pair of samples (506 pairs in all, when self-self comparisons are excluded). When all of the calculated correlations are placed in a sample distance matrix and colored based on the level of similarity, samples that are similar (with no major change in gene expression between them) are nearly the same shade, and large-scale shifts in gene expression appear as sharp changes in color. Overall changes in gene expression occurring in a given time interval can thus be visualized directly and can be assessed relative to the differences observed between biological replicates. When we used this technique to visualize the changes in *B. anthracis* gene expression that occurred during infection of the macrophages (Fig. 2), it was apparent that there was one significant transition, which occurred between 1 and 2 h postinfection. After that

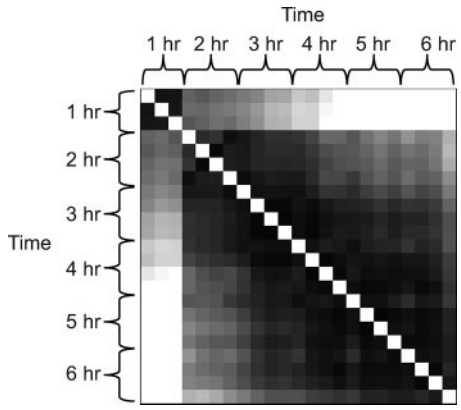

FIG. 2. Sample distance matrix showing the levels of relatedness (as measured by Pearson correlation) between samples isolated from *B. anthracis* growing within murine macrophages at 1, 2, 3, 4, 5, and 6 h postinfection. Samples are organized in the same order in both rows and columns, and the square at the intersection of a given row and a given column is shaded according to the relatedness between the samples (the diagonal is blank, since it represents each sample's comparison to itself). Black indicates a very high degree of similarity between two samples, and progressively lighter shades of gray indicate lower levels of relatedness. White squares indicate a Pearson correlation of <0.6.

point, the samples were extremely similar (that is, the variation between samples collected at neighboring time points was roughly equivalent to the variation observed between samples collected at the same time point).

In order to define the transition between 1 and 2 h postinfection in more detail, we used the SAM algorithm to identify genes whose expression changed significantly between these two points in the time course (54). Consistent with what had been suggested in our sample correlation analysis, we found that nearly 1,100 genes (~19% of the *B. anthracis* Sterne genome) showed a statistically significant change in expression (FDR, <0.001, with at least a twofold change in expression level) between 1 and 2 h postinfection (see Table S1 in the supplemental material). In order to determine the biological implications of this shift in expression pattern, we separated the genes into lists of up- and down-regulated genes and searched these lists for functional families or pathways whose members were statistically overrepresented. We found that in general, genes associated with sporulation/germination and prophage function were down-regulated 1 to 2 h postinfection, while a large number of genes associated with energy metabolism (e.g., the tricarboxylic acid cycle, the pentose phosphate pathway, and glycogen metabolism) were up-regulated (Table 1). Strikingly similar functional trends were observed previously in a recent study that provided a detailed view of the transition between germination/early outgrowth and exponential growth in vitro (6), and the parallels between the two (in vivo and in vitro) seemed to suggest that the transition observed here might be roughly analogous and useful for separating two distinct gene expression programs, one occurring during germination and early outgrowth and the other occurring during the later stages of vegetative growth within the host cell. Consistent with this idea, we noted previously, as well as this study, that intracellular bacteria could first be observed to

TABLE 1. Functional analysis of genes showing a statistically significant change in expression level between 1 and 2 h postinfection

Functional family or pathway	No. of genes in group	No. of genes in *B. anthracis* genome	Statistical significance (*P* value)[c]
Down-regulated genes[a]			
Prophage functions	14	35	8.153E-07
Sporulation and germination	14	54	1.21E-03
Up-regulated genes[b]			
Tricarboxylic acid cycle	11	21	2.122E-06
Energy metabolism	63	295	8.362E-05
Biotin biosynthesis	7	11	1.379E-04
Pantothenate and coenzyme A biosynthesis	5	8	8.818E-04
Electron transport	19	70	1.608E-03
Phosphate transport	5	9	4.143E-03
Biosynthesis of cofactors, prosthetic groups, and carriers	28	130	5.824E-03
Glycogen biosynthesis	3	4	9.861E-03
Purine ribonucleotide biosynthesis	6	15	1.28E-02
Pentose phosphate pathway	4	8	1.356E-02
Response to stress	4	9	2.701E-02
Protein fate	26	131	3.331E-02
Protein secretion	7	23	3.332E-02

[a] Overrepresented functional families and pathways for the genes that were down-regulated during the transition.
[b] Overrepresented families for the genes that were up-regulated.
[c] Statistical significance was calculated using the Fisher exact test.

TABLE 2. Functional analysis of genes showing statistically significant up- or down-regulation during germination and early outgrowth in host macrophages relative to germination and early outgrowth in vitro

Functional family or pathway	No. of genes in group	No. of genes in *B. anthracis* genome	Statistical significance (*P* value)[c]
Down-regulated genes[a]			
Unknown function	193	642	3.232E-06
DNA interactions and regulation of transcription	50	225	4.244E-06
tRNA and rRNA base modification	5	21	3.98E-02
Up-regulated genes[b]			
Purine ribonucleotide biosynthesis	9	15	3.432E-17
Siderophore biosynthesis	5	11	1.169E-09

[a] Overrepresented functional families and pathways for the genes that were down-regulated within the macrophage.
[b] Overrepresented families present in the genes that were up-regulated inside the macrophage.
[c] Statistical significance was calculated using the Fisher exact test.

stain consistently (which occurs only after the start of germination) at roughly 1 h postinfection and bacterial replication could easily be seen approximately 1 h later (7; N. H. Bergman and P. C. Hanna, unpublished data).

Comparison of germination and early outgrowth gene expression patterns in vivo and in vitro. Since the gene expression programs observed before and after the 1- to 2-h transition were quite different (as were the germination/early outgrowth and log-phase expression patterns previously observed in vitro), we chose to examine them separately in more detail, and we were particularly interested in comparing each program observed in vivo (i.e., within the macrophage) to its counterpart in vitro (i.e., in a typical bacterial broth culture). Conveniently, previous work defined the gene expression patterns occurring throughout the entire *B. anthracis* life cycle in vitro (6), and since those experiments used the microarray design that was used here, we were able to make direct comparisons between the data sets. We began our analysis by comparing the samples collected from bacteria within macrophages 1 h postinfection to samples collected during the first 30 min after inoculation of spores into a defined growth medium. The latter samples were essentially the samples collected during the time frame in which the first of five large waves of gene expression occurred during the *B. anthracis* life cycle (6). Several attributes suggested that these samples were the most analogous to the 1-h postinfection samples in terms of growth phase (and thus the comparison between the groups was valid and likely to provide a realistic view of in vivo-specific *B. anthracis* gene expression). The samples collected in the first 30 min of in vitro growth are quite similar to each other, and as in the case of the samples isolated from intracellular bacteria 1 h postinfection, there is a sharp transition in expression pattern between the last of these samples and the next sample in the time course. As we noted earlier, the general trends observed within the two transitions are strikingly similar (Table 1) (6). Finally, of all the samples collected during growth in vitro, these samples are the samples most related to the 1-h in vivo samples, as measured by genome-wide Pearson correlation.

Using SAM to identify differentially expressed genes and EASE to identify biological themes within the sets of genes, our comparison of germination/early outgrowth-associated expression patterns in vivo and in vitro revealed that although these programs are somewhat similar, there are also some notable differences. Relative to expression during germination and early outgrowth inside macrophages, there were 492 genes that were more highly expressed in vitro (expression was >2-fold higher, with an FDR of <0.001) (listed in Table S2 in the supplemental material), yet EASE analysis showed that there were only a few functional families whose members were overrepresented within this set (Table 2). Nearly 40% (193) of these genes are hypothetical or have an unknown function, and in fact this is the single most overrepresented family within the set (note that the Fisher exact test takes overall family size into account when calculating the statistical significance of each observed overrepresentation, so although this is also one of the largest families of genes in the *B. anthracis* genome, the overrepresentation noted for this family remains statistically significant). One other general category—transcriptional regulators—was also heavily overrepresented, with 50 members expressed at significantly higher levels in vitro. As with the hypothetical loci, the precise function of each of these regulatory genes remains unknown, and it appears that if there is an overarching biological difference between the gene expression patterns used by *B. anthracis* during germination and early outgrowth in vitro and in vivo, it may simply be that the expression program used in vivo is much less complex, and perhaps more parsimonious, than the one used in vitro. Perhaps this reflects the fact that the intracellular environment is rela-

tively rich relative to the in vitro growth conditions and the bacterial cell must make fewer adaptations to its environment.

Consistent with this idea, only 40 genes were more highly expressed when germination and early outgrowth took place within the host macrophage (see Table S2 in the supplemental material), and these genes tended to be involved in a small number of highly overrepresented pathways or processes (Table 2). Notably, the loci involved in de novo purine biosynthesis, as well as genes encoding enzymes utilized by the cell in synthesizing both *B. anthracis* siderophores, were all expressed at much higher levels (>5-fold) within the macrophage than in vitro. It should be noted that neither purines nor iron is present at high concentrations in the modified G medium that the in vitro cultures were grown in (this medium, while not minimal, is relatively nutrient poor) so the higher expression levels of these genes seems to suggest that conditions within the macrophage are limiting for both purines and iron. Similar findings have been reported in other studies of intracellular bacterial pathogens (11, 12, 19, 39), and collectively, the previous reports and this study suggest that both purine biosynthesis and iron acquisition may be pathways that contain potentially useful drug targets.

Interestingly, the small set of 40 genes also included a number of genes that have previously been shown to play a role in virulence (it is difficult to place an estimate on the statistical significance of this observation, because pathogenesis is a loosely defined functional family, and it is not clear how many [and which] of the >5,800 *B. anthracis* genes are involved in causing disease). These genes included *lef* (encoding lethal factor), *pagA* (encoding protective antigen), and *pagR* (encoding a regulator known to activate transcription of the toxin subunit genes), as well as other genes, like *katB*, a catalase gene with homologs in other species that have been shown to be involved in protecting the bacterium from host-derived reactive oxygen intermediates (2, 3). Our finding that these genes are highly up-regulated in vivo indicates that expression of these virulence factors is not simply a preprogrammed part of a "universal" germination/early outgrowth expression program but rather a specific response to one or more environmental cues present in the intracellular environment (perhaps CO_2, which has been shown to induce the expression of toxin components [14, 27, 28]). The data also highlight the alacrity of this response; earlier studies reported that the *B. anthracis* toxin genes are induced within the first 3 h inside the macrophage (4, 25, 26), and our results extend these findings by showing that even within the first hour of growth in vivo, before it has fully begun vegetative growth, *B. anthracis* is capable of initiating pathogenesis (that is, changing its global gene expression patterns in response to the intracellular environment).

Comparison of *B. anthracis* gene expression patterns during later stages of growth in vivo and in vitro. Since we had observed that the gene expression program used by *B. anthracis* during the later stages of vegetative growth differs significantly from the program used during germination and early outgrowth (both in vitro and in vivo), we were interested to see how the specific adaptations to the macrophage environment that we observed during the earliest stages of growth fit into the bacterium's long-term strategy for surviving within, and eventually killing, the host macrophage. As noted above, our initial analysis of expression in vivo showed that the samples collected from 2 to 6 h postinfection were very similar; in fact, when we measured genome-wide Pearson correlations for all 380 possible pairs within this subset of samples, we found that even the most distantly related samples had a correlation of >0.88, and most pairs had a correlation of >0.95. Based on the fact that these samples were collected immediately following a shift in gene expression that appeared to signal the cells' transition from germination and early outgrowth to normal vegetative growth, we expected that the samples collected from within macrophages 2 to 6 h postinfection would be somewhat similar to samples collected during vegetative growth in vitro. Correlation analysis showed that the nearest "relatives" of these samples were indeed the samples isolated from cells growing in a log-phase culture in vitro (the time frame in which the second of the five waves described by Bergman et al. [6] was expressed, roughly 30 to 210 min after inoculation), and it appears that the two sets of samples represent similar phases of growth, albeit in very different environments.

In order to identify the differences between in vivo and in vitro vegetative growth expression patterns, we performed a SAM comparing the 20 samples collected 2, 3, 4, 5, and 6 h postinfection to samples collected during vegetative growth in vitro (19 samples in all, collected from 30 to 210 min after inoculation). Like the samples collected in vivo, the samples isolated during vegetative growth in vitro were very similar to each other, and overall the group was clearly defined by sharp transitions in genome-wide expression patterns both before and after vegetative growth (6). There were 1,551 genes that showed significant differential expression in the in vivo and in vitro samples; 1,052 loci were expressed at lower levels in vivo, and 448 loci were more highly expressed during growth within the macrophage (see Table S3 in the supplemental material).

TABLE 3. Functional analysis of genes showing statistically significant up- or down-regulation during the later stages of growth within host macrophages relative to growth in vitro

Functional family or pathway	No. of genes in group	No. of genes in *B. anthracis* genome	Statistical significance (*P* value)[c]
Down-regulated genes[a]			
Chemotaxis and motility	26	41	8.919E-11
Histidine biosynthesis	9	10	1.001E-06
Unknown function	337	642	5.169E-04
Signal transduction/ two-component systems	36	92	5.205E-04
Phosphate transport	4	9	3.641E-03
Potassium ion transport	5	7	5.087E-03
Structural constituent of cell wall	7	17	1.648E-02
Up-regulated genes[b]			
Iron acquisition	28	54	1.557E-15
Purine ribonucleotide biosynthesis	13	15	1.12E-12
Biotin biosynthesis	8	11	1.441E-07
Arginine biosynthesis	7	9	5.188E-07
Nitrate reductase activity	3	4	1.772E-03
Anaerobic electron transport	3	4	1.772E-03
NADH metabolism/ nicotinamide synthesis	3	5	4.173E-03

[a] Overrepresented functional families and pathways for the genes that were down-regulated within the macrophage.
[b] Overrepresented families for the genes that were up-regulated inside the macrophage.
[c] Statistical significance was calculated using the Fisher exact test.

TABLE 4. Fifty *B. anthracis* genes most highly up-regulated during growth in host macrophages relative to growth in vitro

Gene (*B. anthracis* Ames Ancestor genome)[a]	Common name[b]	Fold change (in vivo/in vitro)	Functional family[c]
GBAA5564	Conserved hypothetical protein	66.56	Hypothetical proteins
GBAA4660	*nadA* (quinolinate synthetase complex, subunit A)	36.84	Biosynthesis of cofactors, prosthetic groups, and carriers
GBAA1908	Conserved hypothetical protein	32.14	Hypothetical proteins
GBAA4661	*nadC* (nicotinate-nucleotide pyrophosphorylase, carboxylating)	26.51	Biosynthesis of cofactors, prosthetic groups, and carriers
GBAA2368	*entA* (2,3-dihydro-2,3-dihydroxybenzoate dehydrogenase)	24.78	Biosynthesis of cofactors, prosthetic groups, and carriers
GBAA3704	Glyoxylase family protein	24.29	Unknown function
GBAA5668	Major facilitator family transporter	23.93	Transport and binding proteins
GBAA1917	Rrf2 family protein	21.78	Unknown function
GBAA3730	Conserved hypothetical protein	21.29	Hypothetical proteins
GBAA3191	ABC transporter, ATP-binding protein	21.06	Transport and binding proteins
GBAA5150	BioY family protein	19.99	Biosynthesis of cofactors, prosthetic groups, and carriers
GBAA3596	Flavodoxin	19.58	Energy metabolism
GBAA3595	BNR repeat domain protein	18.17	Unknown function
GBAA4662	*nadB* (L-aspartate oxidase)	18.09	Biosynthesis of cofactors, prosthetic groups, and carriers
GBAA1158	*hemH-2* (ferrochelatase)	15.78	Biosynthesis of cofactors, prosthetic groups, and carriers
GBAA0827	Conserved hypothetical protein	15.45	Hypothetical proteins
GBAA1159	*katB* (catalase)	14.58	Cellular processes
GBAA1019	Hydrolase, alpha/beta fold family	14.05	Unknown function
GBAA5284	Transcriptional regulator, MarR family	13.64	Regulatory functions
GBAA4340	*bioD* (dethiobiotin synthetase)	13.25	Biosynthesis of cofactors, prosthetic groups, and carriers
GBAA0689	Proton/peptide symporter family protein	12.65	Transport and binding proteins
GBAA3867	Iron compound ABC transporter, iron compound-binding protein	12.46	Transport and binding proteins
GBAA1015	Glyoxalase family protein	12.41	Unknown function
GBAA4341	*bioA* (adenosylmethionine–8-amino-7-oxononanoate aminotransferase)	12.31	Biosynthesis of cofactors, prosthetic groups, and carriers
GBAA5696	*sodA-2* (superoxide dismutase, Mn)	12.27	Cellular processes
GBAA3456	Conserved hypothetical protein	12.04	Hypothetical proteins
GBAA3190	ABC transporter, permease protein	11.93	Transport and binding proteins
GBAA3703	Phospholipase/carboxylesterase family protein	11.78	Unknown function
GBAA0296	*purM* (phosphoribosylformylglycinamidine cyclo-ligase PF02769)	11.58	Purines, pyrimidines, nucleosides, and nucleotides
GBAA1394	Flavodoxin	11.31	Energy metabolism
GBAA4339	*bioF* (8-amino-7-oxononanoate synthase)	11.29	Biosynthesis of cofactors, prosthetic groups, and carriers
GBAA3731	Membrane protein, putative	11.20	Cell envelope
GBAA1941	Transcriptional regulator, MarR family	11.02	Regulatory functions
GBAA4338	BioH protein	10.81	Biosynthesis of cofactors, prosthetic groups, and carriers
GBAA1395	Hypothetical protein	10.75	
GBAA3455	Hypothetical protein	10.65	
GBAA0297	*purN* (phosphoribosylglycinamide formyltransferase)	10.61	Purines, pyrimidines, nucleosides, and nucleotides
GBAA4597	Iron compound ABC transporter, iron compound-binding protein	10.60	Transport and binding proteins
GBAA3454	Hypothetical protein	10.47	
GBAA_pXO1_0171	RNase domain protein	10.38	
GBAA1020	Conserved hypothetical protein	10.29	Hypothetical proteins
GBAA4663	Aminotransferase, class V	10.27	Unknown function
GBAA5302	Conserved hypothetical protein	10.21	Hypothetical proteins
GBAA4813	Conserved hypothetical protein	10.15	Hypothetical proteins
GBAA0866	*alsS* (acetolactate synthase)	9.70	Energy metabolism
GBAA0293	*purQ* (phosphoribosylformylglycinamidine synthase I)	9.56	Purines, pyrimidines, nucleosides, and nucleotides
GBAA5283	Conserved hypothetical protein	9.47	Hypothetical proteins
GBAA4336	*bioB* (biotin synthetase)	9.35	Biosynthesis of cofactors, prosthetic groups, and carriers
GBAA1918	2-Hydroxychromene-2-carboxylate isomerase family protein	9.34	Unknown function
GBAA4337	Biotin synthesis protein BioC	9.18	Biosynthesis of cofactors, prosthetic groups, and carriers

[a] Genes were identified using SAM, with a FDR of <0.001 and a required fold change of >2.00.
[b] The common names are those assigned during annotation of the *B. anthracis* Ames Ancestor genome (GenBank accession no. AE017334).
[c] Functional family assignments are based on the TIGR role categories currently assigned to *B. anthracis* genes in the Comprehensive Microbial Resource (http://cmr.tigr.org).

As we observed in our analysis of germination and early outgrowth, the set of genes that were expressed at lower levels in vivo included a large number (337) of loci that are hypothetical or have an unknown function (Table 3). Similarly, a number of genes encoding regulatory proteins were also found within this set. These findings, together with the fact that in both early and later stages of growth in vivo the repressed genes far outnumber the induced genes, seem to lend credence

TABLE 5. Comparison of fold changes using microarray and quantitative RT-PCR[a]

B. anthracis gene	Common name	Fold change (microarray)	Fold change (quantitative RT-PCR)
pXO1_166	*pagR* (transcriptional repressor)	2.82	3.03
pXO1_172	*lef* (lethal factor)	3.13	3.55
GBAA0226	Hypothetical protein	−0.28	−0.25
GBAA0295	*purF* (amidophosphoribosyltransferase)	3.18	3.79
GBAA0797	ABC transporter, permease protein	−0.44	−0.77
GBAA1159	*katB* (catalase)	3.86	3.53
GBAA2368	*entA* (2,3-dihydro-2,3-dihydroxybenzoate dehydrogenase)	4.63	5.26
GBAA4660	*nadA* (quinolinate synthetase complex, subunit A)	5.20	4.36
GBAA4788	Conserved domain protein	3.00	3.14
GBAA5490	Hypothetical protein	−1.31	−0.97

[a] Fold changes are expressed as the $\log_2$ of the ratio of a gene's expression level during growth within the host macrophage to its expression level during growth in vitro.

to the idea that within the macrophage, *B. anthracis* gene expression follows a more parsimonious program. This idea also seems intuitive given the different growth rates in vivo and in vitro. A combination of direct (microscopy-based counting) and indirect (CFU-based) methods has shown that in the model infection system used for this study, the intracellular bacteria go through only one or two replication cycles before killing the macrophages at roughly 6 h postinfection (data not shown), which means that their growth rate is significantly lower than what is usually observed in vitro (where *B. anthracis* doubling times are typically less than 30 min [44]).

The lower growth rate of *B. anthracis* in vivo also explains some of the other overrepresented functional families within the set of genes that are expressed at lower levels in vivo. For instance, the most statistically significant overrepresentation occurred in the family of genes related to chemotaxis and motility; 26 members of this family were repressed in vivo relative to their expression during growth in vitro. In *Bacillus subtilis*, these genes are expressed during rapid growth (41), and their repression in *B. anthracis* cells growing in vivo seems to be consistent with a much lower growth rate inside the host cells (note that although *B. anthracis* is known to be nonmotile, this is because of several frameshift mutations within the flagellar genes [47]; the genes are otherwise intact, and previous studies have shown that their regulation appears to mirror the trends observed in *B. subtilis* [6, 38]). Similarly, the repression in vivo of a family of genes involved in cell wall synthesis points to a lower rate of cell division within the host phagocyte.

Among the *B. anthracis* genes that were more highly expressed in vivo (the 50 most highly induced genes are shown in Table 4, and a complete list is shown in Table S3 in the supplemental material), we found many of the same loci that had been induced during germination and early outgrowth in vivo, and their induction in the later stages of growth within the macrophage was even more pronounced. The families of genes involved in both iron acquisition and purine biosynthesis continued to be highly overrepresented (Table 3), and some of these genes were expressed in vivo at levels that were 20-fold or more greater than their expression levels during vegetative growth in vitro. In addition, *B. anthracis* also appeared to make a number of further metabolic adaptations to the intracellular environment; genes involved in the biosynthesis of several amino acids (notably arginine), biotin, and NAD were all overrepresented within this group, and, as observed with purine biosynthesis and iron acquisition, many of these genes were expressed at much higher levels in vivo than in vitro (the NAD biosynthetic loci *nadA*, *nadB*, and *nadC*, for instance, were induced 18- to 37-fold). Finally, we also noted that the bacterium appears to be oxygen starved within the macrophage, as a number of genes associated with the use of alternate electron acceptors were up-regulated as well.

Overall, it appeared from our data that in the later stages of growth within the macrophage, *B. anthracis* made a more profound change in gene expression in order to more fully adapt to the intracellular environment, and this trend was also borne out in our examination of known virulence-associated genes. Whereas during the earliest stages of growth a somewhat limited set of these genes was induced in vivo, in the later stages we found a much larger number of known virulence factors up-regulated within the macrophage. These genes included the toxin genes *lef*, *pagA*, and *cya* (1), the regulatory loci *atxA* and *pagR* (22), *srtB* encoding sortase (58), and siderophore biosynthesis genes (11), as well as numerous genes that have not been characterized yet in *B. anthracis* but have homologs in other species that have been linked to virulence. Examples of the last set include genes encoding a hemolysin, several phospholipases, and adhesion lipoproteins and the catalase gene *katB*, as well as genes encoding several members of a multidrug resistance protein family, and it will be of considerable interest to characterize these genes in more detail and determine the extent to which they may be involved in virulence.

Looking beyond the genes that have previously been linked to pathogenesis, the genome-wide expression data presented in this study also allowed us to identify a number of loci that have been ignored until now but appear to be worthy of further investigation. For instance, 13 of the 50 most induced genes during growth within the host macrophage are hypothetical, yet some of these genes are expressed in vivo at levels that are 20-, 30-, or 50-fold above their expression levels during growth in vitro. Similarly, for many of the other highly induced *B. anthracis* genes only a general function has been assigned (e.g., a glyoxylase family protein or a membrane protein), and although the precise roles of these genes remain a mystery, their expression profiles suggest that they may be important for survival within the host cell. In some ways, these genes provide some of the most interesting leads for future research in an-

thrax, if only because they hint at previously unappreciated aspects of *B. anthracis* pathogenesis.

Validation of microarray data by quantitative RT-PCR. Prior to beginning any further experiments aimed at characterizing individual genes in detail, we sought to validate the expression trends noted above by comparing our microarray results to data obtained using an alternate method. This was particularly important given that although it seemed unlikely, it was possible that the addition of the differential lysis and MicrobEnrich steps to our standard RNA extraction procedure may have resulted in the selective enrichment of a subset of transcripts and thus confounded our analysis of the microarray data. We therefore prepared RNA from cells grown in vitro (log-phase culture at an optical density at 600 nm of ~0.3, growing with rapid shaking in modified G medium) and in vivo (within murine macrophages, 4 h postinfection), using the same basic extraction procedure in each case (essentially as described previously [6] and without the differential lysis and MicrobEnrich steps), and used these samples as test samples. We chose a representative group of genes from the *B. anthracis* genome, including genes that the microarray data suggested were highly induced during growth within the macrophage, as well as other genes that showed little change or slight down-regulation in vivo, and we used quantitative RT-PCR to measure the changes in expression level between growth in vitro and growth within the macrophage. The data were collected as described in Materials and Methods and are shown in Table 5 along with the corresponding measurements taken from the microarray data. Overall, the fold change measurements obtained from quantitative RT-PCR experiments matched quite closely their microarray counterparts; there was no obvious bias in either direction (that is, in terms of one method overestimating differential expression relative to the other), and a Deming linear regression of the two sets of measurements resulted in a slope of 0.97 ± 0.067, where a slope of 1.0 indicates perfect agreement. Given this level of concordance, it seems very likely that the microarray data presented in this study do in fact reflect changes in transcript abundance between *B. anthracis* growing in vitro and *B. anthracis* growing in vivo.

Individual characterization of GBAA1941 and its role in pathogenesis. As noted above, the microarray data identified a number of highly interesting genes that have not been characterized yet but appear to be significantly up-regulated during infection of the host macrophage. Among these genes are several putative regulatory genes, and we chose one (GBAA1941) for further characterization because its product shares significant homology with a family of transcriptional regulators (MarR) known to play roles in ligand-mediated regulation of virulence factor production and bacterial responses to environment stress (56). Furthermore, members of this family have been shown to be critical for virulence in a variety of bacterial pathogens, including *Staphylococcus aureus* (31), *Xanthomonas campestris* (55), *Erwinia chrysanthemi* (49), and *Yersinia pestis* (10). Transcription of GBAA1941 is up-regulated more than 10-fold during growth within the macrophage, and we sought to test whether this expression profile might in fact reflect a prominent role for this locus in *B. anthracis* pathogenesis. We constructed an isogenic strain of *B. anthracis* in which GBAA1941 was deleted and characterized this strain to determine its ability to grow in vitro and its ability to cause disease in a mouse model of inhalational anthrax. We found that the growth rates and final cell densities for the Sterne $34F_2$ parent strain and the ΔGBAA1941 mutant strain were essentially indistinguishable in both brain heart infusion and modified G media, and sporulation of the mutant strain also appeared to be normal. In the murine model of inhalational anthrax, however, the two strains behaved very differently. Figure 3 shows survival curves for mice that were inoculated via intratracheal injection with 1.5×10^4 spores of either the parent Sterne $34F_2$ or mutant ΔGBAA1941 strain. This dose of Sterne $34F_2$ spores represents roughly a 90% lethal dose in this model system (21), and only 2 of the original 27 mice in the parent group survived the infection. In contrast, nearly one-half (12 of 26) of the mice inoculated with the mutant strain survived the infection. The difference between the two survival curves is statistically significant ($P = 0.0003$, as calculated by the log rank test), and it indicates that the GBAA1941 locus is in fact important for *B. anthracis* pathogenesis. In a broader sense, these data also validate the approach taken in this study, in that they confirm that microarrays are valuable not only for investigating global transcriptional trends during infection but also for identifying previously uncharacterized virulence-associated genes. It will be of interest to further define the functions of GBAA1941 and the other genes identified in this study, and a number of such experiments are under way in our laboratory.

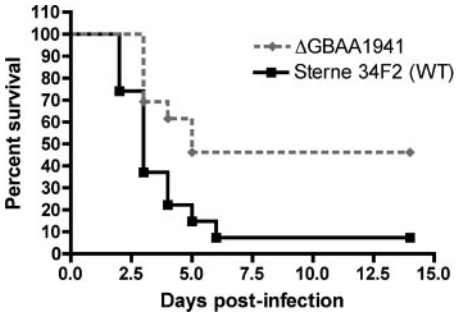

FIG. 3. Survival of mice infected with *B. anthracis* parent (Sterne $34F_2$) and mutant (ΔGBAA1941) strains. DBA/2 mice were inoculated via intratracheal injection of 1.5×10^4 spores of either the parent or mutant strain. The total initial group sizes were 27 mice (parent) and 26 mice (mutant), and the percentage of each group surviving is shown relative to time. A log rank test showed that the difference between the two survival curves is statistically significant, with a P value of 0.0003.

ACKNOWLEDGMENTS

We thank Z. Qin and members of the Hanna laboratory for valuable discussions.

This work was supported by HHS contract N266200400059C-N01-AI-40059.

REFERENCES

1. **Baldari, C., F. Tonello, S. Paccani, and C. Montecucco.** 2006. Anthrax toxins: a paradigm of bacterial immune suppression. Trends Immunol. **27:**434–440.
2. **Bandyopadhyay, P., B. Byrne, Y. Chan, M. S. Swanson, and H. M. Steinman.** 2003. *Legionella pneumophila* catalase-peroxidases are required for proper trafficking and growth in primary macrophages. Infect. Immun. **71:**4526–4535.
3. **Bandyopadhyay, P., and H. M. Steinman.** 1998. *Legionella pneumophila* catalase-peroxidases: cloning of the *katB* gene and studies of KatB function. J. Bacteriol. **180:**5369–5374.

4. **Banks, D. J., M. Barnajian, F. J. Maldonado-Arocho, A. M. Sanchez, and K. A. Bradley.** 2005. Anthrax toxin receptor 2 mediates *Bacillus anthracis* killing of macrophages following spore challenge. Cell. Microbiol. **7:**1173–1185.
5. **Barnes, J.** 1947. The development of anthrax following the administration of spores by inhalation. Br. J. Exp. Pathol **28:**385–394.
6. **Bergman, N. H., E. C. Anderson, E. E. Swenson, M. M. Niemeyer, A. D. Miyoshi, and P. C. Hanna.** 2006. Transcriptional profiling of the *Bacillus anthracis* life cycle in vitro and an implied model for regulation of spore formation. J. Bacteriol. **188:**6092–6100.
7. **Bergman, N. H., K. D. Passalacqua, R. Gaspard, L. M. Shetron-Rama, J. Quackenbush, and P. C. Hanna.** 2005. Murine macrophage transcriptional responses to *Bacillus anthracis* infection and intoxication. Infect. Immun. **73:**1069–1080.
8. **Bolstad, B. M., R. A. Irizarry, M. Astrand, and T. P. Speed.** 2003. A comparison of normalization methods for high density oligonucleotide array data based on variance and bias. Bioinformatics **19:**185–193.
9. **Brittingham, K. C., G. Ruthel, R. G. Panchal, C. L. Fuller, W. J. Ribot, T. A. Hoover, H. A. Young, A. O. Anderson, and S. Bavari.** 2005. Dendritic cells endocytose *Bacillus anthracis* spores: implications for anthrax pathogenesis. J. Immunol. **174:**5545–5552.
10. **Cathelyn, J. S., S. D. Crosby, W. W. Lathem, W. E. Goldman, and V. L. Miller.** 2006. RovA, a global regulator of *Yersinia pestis*, specifically required for bubonic plague. Proc. Natl. Acad. Sci. USA **103:**13514–13519.
11. **Cendrowski, S., W. MacArthur, and P. Hanna.** 2004. *Bacillus anthracis* requires siderophore biosynthesis for growth in macrophages and mouse virulence. Mol. Microbiol. **51:**407–417.
12. **Chatterjee, S. S., H. Hossain, S. Otten, C. Kuenne, K. Kuchmina, S. Machata, E. Domann, T. Chakraborty, and T. Hain.** 2006. Intracellular gene expression profile of *Listeria monocytogenes*. Infect. Immun. **74:**1323–1338.
13. **Cleret, A., A. Quesnel-Hellmann, J. Mathieu, D. Vidal, and J. N. Tournier.** 2006. Resident $CD11c^+$ lung cells are impaired by anthrax toxins after spore infection. J. Infect. Dis. **194:**86–94.
14. **Dai, Z., J. Sirard, M. Mock, and T. Koehler.** 1995. The *atxA* gene product activates transcription of the anthrax toxin genes and is essential for virulence. Mol. Microbiol. **16:**1171–1181.
15. **Dixon, T., A. Fahd, T. Koehler, J. Swanson, and P. Hanna.** 2000. Early events in anthrax pathogenesis: intracellular survival of *B. anthracis* and its escape from RAW264.7 macrophages. Cell. Microbiol. **2:**453–463.
16. **Dixon, T., M. Meselson, J. Guillemin, and P. Hanna.** 1999. Medical progress: anthrax. N. Engl. J. Med. **341:**815–826.
17. **Drysdale, M., S. Heninger, J. Hutt, Y. Chen, C. R. Lyons, and T. M. Koehler.** 2005. Capsule synthesis by *Bacillus anthracis* is required for dissemination in murine inhalation anthrax. EMBO J. **24:**221–227.
18. **Du, Y., J. Lenz, and C. G. Arvidson.** 2005. Global gene expression and the role of sigma factors in *Neisseria gonorrhoeae* in interactions with epithelial cells. Infect. Immun. **73:**4834–4845.
19. **Eriksson, S., S. Lucchini, A. Thompson, M. Rhen, and J. C. Hinton.** 2003. Unravelling the biology of macrophage infection by gene expression profiling of intracellular *Salmonella enterica*. Mol. Microbiol. **47:**103–118.
20. **Ezzell, J. W., and S. L. Welkos.** 1999. The capsule of *Bacillus anthracis*, a review. J. Appl. Microbiol. **87:**250.
21. **Fisher, N., L. Shetron-Rama, A. Herring-Palmer, B. Heffernan, N. Bergman, and P. Hanna.** 2006. The *dltABCD* operon of *Bacillus anthracis* Sterne is required for virulence and resistance to peptide, enzymatic, and cellular mediators of innate immunity. J. Bacteriol. **188:**1301–1309.
22. **Fouet, A., and M. Mock.** 2006. Regulatory networks for virulence and persistence of *Bacillus anthracis*. Curr. Opin. Microbiol. **9:**160–166.
23. **Fritz, D. L., N. K. Jaax, W. B. Lawrence, K. J. Davis, M. L. Pitt, J. W. Ezzell, and A. M. Friedlander.** 1995. Pathology of experimental inhalation anthrax in the rhesus monkey. Lab. Investig. **73:**691–702.
24. **Guarner, J., J. A. Jernigan, W. J. Shieh, K. Tatti, L. M. Flannagan, D. S. Stephens, T. Popovic, D. A. Ashford, B. A. Perkins, and S. R. Zaki.** 2003. Pathology and pathogenesis of bioterrorism-related inhalational anthrax. Am. J. Pathol. **163:**701–709.
25. **Guidi-Rontani, C., M. Levy, H. Ohayon, and M. Mock.** 2001. Fate of germinated *Bacillus anthracis* spores in primary murine macrophages. Mol. Microbiol. **42:**931–938.
26. **Guidi-Rontani, C., M. Weber-Levy, E. Labruyere, and M. Mock.** 1999. Germination of *Bacillus anthracis* spores within alveolar macrophages. Mol. Microbiol. **31:**9–17.
27. **Hoffmaster, A. R., and T. M. Koehler.** 1997. The anthrax toxin activator gene *atxA* is associated with CO_2-enhanced non-toxin gene expression in *Bacillus anthracis*. Infect. Immun. **65:**3091–3099.
28. **Hoffmaster, A. R., and T. M. Koehler.** 1999. Control of virulence gene expression in *Bacillus anthracis*. J. Appl. Microbiol. **87:**279–281.
29. **Hornstra, L. M., Y. P. de Vries, W. M. de Vos, and T. Abee.** 2006. Influence of sporulation medium composition on transcription of *ger* operons and the germination response of spores of *Bacillus cereus* ATCC 14579. Appl. Environ. Microbiol. **72:**3746–3749.
30. **Hosack, D. A., G. Dennis, Jr., B. T. Sherman, H. C. Lane, and R. A. Lempicki.** 2003. Identifying biological themes within lists of genes with EASE. Genome Biol. **4:**R70.
31. **Ingavale, S., W. van Wamel, T. T. Luong, C. Y. Lee, and A. L. Cheung.** 2005. Rat/MgrA, a regulator of autolysis, is a regulator of virulence genes in *Staphylococcus aureus*. Infect. Immun. **73:**1423–1431.
32. **Irizarry, R. A., B. M. Bolstad, F. Collin, L. M. Cope, B. Hobbs, and T. P. Speed.** 2003. Summaries of Affymetrix GeneChip probe level data. Nucleic Acids Res. **31:**e15.
33. **Irizarry, R. A., B. Hobbs, F. Collin, Y. D. Beazer-Barclay, K. J. Antonellis, U. Scherf, and T. P. Speed.** 2003. Exploration, normalization, and summaries of high density oligonucleotide array probe level data. Biostatistics **4:**249–264.
34. **Janes, B. K., and S. Stibitz.** 2006. Routine markerless gene replacement in *Bacillus anthracis*. Infect. Immun. **74:**1949–1953.
35. **Jernigan, J. A., D. S. Stephens, D. A. Ashford, C. Omenaca, M. S. Topiel, M. Galbraith, M. Tapper, T. L. Fisk, S. Zaki, T. Popovic, R. F. Meyer, C. P. Quinn, S. A. Harper, S. K. Fridkin, J. J. Sejvar, C. W. Shepard, M. McConnell, J. Guarner, W. J. Shieh, J. M. Malecki, J. L. Gerberding, J. M. Hughes, and B. A. Perkins.** 2001. Bioterrorism-related inhalational anthrax: the first 10 cases reported in the United States. Emerg. Infect. Dis. **7:**933–944.
36. **Kim, H. U., and J. M. Goepfert.** 1974. A sporulation medium for *Bacillus anthracis*. J. Appl. Bacteriol. **37:**265–267.
37. **Lee, J. Y., B. K. Janes, K. D. Passalacqua, B. F. Pfleger, N. H. Bergman, H. Liu, K. Hakansson, R. V. Somu, C. C. Aldrich, S. Cendrowski, P. C. Hanna, and D. H. Sherman.** 2007. Biosynthetic analysis of the petrobactin siderophore pathway from *Bacillus anthracis*. J. Bacteriol. **189:**1698–1710.
38. **Liu, H., N. H. Bergman, B. Thomason, S. Shallom, A. Hazen, J. Crossno, D. A. Rasko, J. Ravel, T. D. Read, S. N. Peterson, J. Yates III, and P. C. Hanna.** 2004. Formation and composition of the *Bacillus anthracis* endospore. J Bacteriol. **186:**164–178.
39. **Lucchini, S., H. Liu, Q. Jin, J. C. Hinton, and J. Yu.** 2005. Transcriptional adaptation of *Shigella flexneri* during infection of macrophages and epithelial cells: insights into the strategies of a cytosolic bacterial pathogen. Infect. Immun. **73:**88–102.
40. **Lyons, C. R., J. Lovchik, J. Hutt, M. F. Lipscomb, E. Wang, S. Heninger, L. Berliba, and K. Garrison.** 2004. Murine model of pulmonary anthrax: kinetics of dissemination, histopathology, and mouse strain susceptibility. Infect. Immun. **72:**4801–4809.
41. **Marquez, L. M., J. D. Helmann, E. Ferrari, H. M. Parker, G. W. Ordal, and M. J. Chamberlin.** 1990. Studies of sigma D-dependent functions in *Bacillus subtilis*. J. Bacteriol. **172:**3435–3443.
42. **Nicholson, W. L., N. Munakata, G. Horneck, H. J. Melosh, and P. Setlow.** 2000. Resistance of *Bacillus* endospores to extreme terrestrial and extraterrestrial environments. Microbiol. Mol. Biol. Rev. **64:**548–572.
43. **Passalacqua, K. D., and N. H. Bergman.** 2006. *Bacillus anthracis*: interactions with the host and establishment of inhalational anthrax. Future Microbiol. **1:**397–415.
44. **Passalacqua, K. D., N. H. Bergman, A. Herring-Palmer, and P. Hanna.** 2006. The superoxide dismutases of *Bacillus anthracis* do not cooperatively protect against endogenous superoxide stress. J. Bacteriol. **188:**3837–3848.
45. **Pickering, A., and T. Merkel.** 2004. Macrophages release tumor necrosis factor alpha and interleukin-12 in response to intracellular *Bacillus anthracis* spores. Infect. Immun. **72:**3069–3072.
46. **Pickering, A. K., M. Osorio, G. M. Lee, V. K. Grippe, M. Bray, and T. J. Merkel.** 2004. Cytokine response to infection with *Bacillus anthracis* spores. Infect. Immun. **72:**6382–6389.
47. **Read, T. D., S. N. Peterson, N. Tourasse, L. W. Baillie, I. T. Paulsen, K. E. Nelson, H. Tettelin, D. E. Fouts, J. A. Eisen, S. R. Gill, E. Holtzapple, O. A. Okstad, E. Helgason, J. Rilstone, M. Wu, J. F. Kolonay, M. J. Beanan, R. J. Dodson, L. M. Brinkac, M. Gwinn, R. T. DeBoy, R. Madpu, S. C. Daugherty, A. S. Durkin, D. H. Haft, W. C. Nelson, J. D. Peterson, M. Pop, H. M. Khouri, D. Radune, J. L. Benton, Y. Mahamoud, L. Jiang, I. R. Hance, J. F. Weidman, K. J. Berry, R. D. Plaut, A. M. Wolf, K. L. Watkins, W. C. Nierman, A. Hazen, R. Cline, C. Redmond, J. E. Thwaite, O. White, S. L. Salzberg, B. Thomason, A. M. Friedlander, T. M. Koehler, P. C. Hanna, A. B. Kolsto, and C. M. Fraser.** 2003. The genome sequence of *Bacillus anthracis* Ames and comparison to closely-related bacteria. Nature **423:**81–86.
48. **Ross, J.** 1957. The pathogenesis of anthrax following the administration of spores by the respiratory route. J. Pathol. Bacteriol. **73:**485–494.
49. **Rouanet, C., S. Reverchon, D. A. Rodionov, and W. Nasser.** 2004. Definition of a consensus DNA-binding site for PecS, a global regulator of virulence gene expression in *Erwinia chrysanthemi* and identification of new members of the PecS regulon. J. Biol. Chem. **279:**30158–30167.
50. **Ruthel, G., W. J. Ribot, S. Bavari, and T. A. Hoover.** 2004. Time-lapse confocal imaging of development of *Bacillus anthracis* in macrophages. J. Infect. Dis. **189:**1313–1316.
51. **Saeed, A. I., V. Sharov, J. White, J. Li, W. Liang, N. Bhagabati, J. Braisted, M. Klapa, T. Currier, M. Thiagarajan, A. Sturn, M. Snuffin, A. Rezantsev, D. Popov, A. Ryltsov, E. Kostukovich, I. Borisovsky, Z. Liu, A. Vinsavich, V. Trush, and J. Quackenbush.** 2003. TM4: a free, open-source system for microarray data management and analysis. BioTechniques **34:**374–378.

52. **Shafazand, S., R. Doyle, S. Ruoss, A. Weinacker, and T. A. Raffin.** 1999. Inhalational anthrax: epidemiology, diagnosis, and management. Chest **116:** 1369–1376.
53. **Tournier, J. N., A. Quesnel-Hellmann, J. Mathieu, C. Montecucco, W. J. Tang, M. Mock, D. R. Vidal, and P. L. Goossens.** 2005. Anthrax edema toxin cooperates with lethal toxin to impair cytokine secretion during infection of dendritic cells. J. Immunol. **174:**4934–4941.
54. **Tusher, V. G., R. Tibshirani, and G. Chu.** 2001. Significance analysis of microarrays applied to the ionizing radiation response. Proc. Natl. Acad. Sci. USA **98:**5116–5121.
55. **Wei, K., D. J. Tang, Y. Q. He, J. X. Feng, B. L. Jiang, G. T. Lu, B. Chen, and J. L. Tang.** 2007. *hpaR*, a putative *marR* family transcriptional regulator, is positively controlled by HrpG and HrpX and involved in the pathogenesis, hypersensitive response, and extracellular protease production of *Xanthomonas campestris* pathovar *campestris*. J. Bacteriol. **189:** 2055–2062.
56. **Wilkinson, S. P., and A. Grove.** 2006. Ligand-responsive transcriptional regulation by members of the MarR family of winged helix proteins. Curr. Issues Mol. Biol. **8:**51–62.
57. **Zaucha, G. M., L. M. Pitt, J. Estep, B. E. Ivins, and A. M. Friedlander.** 1998. The pathology of experimental anthrax in rabbits exposed by inhalation and subcutaneous inoculation. Arch. Pathol. Lab. Med. **122:**982–992.
58. **Zink, S. D., and D. L. Burns.** 2005. Importance of *srtA* and *srtB* for growth of *Bacillus anthracis* in macrophages. Infect. Immun. **73:**5222–5228.

Editor: J. B. Bliska